



Growth front nucleation of rubrene thin films for high mobility organic transistors

C. H. Hsu, J. Deng, C. R. Staddon, and P. H. Beton

Citation: [Applied Physics Letters](#) **91**, 193505 (2007); doi: 10.1063/1.2805030

View online: <http://dx.doi.org/10.1063/1.2805030>

View Table of Contents: <http://scitation.aip.org/content/aip/journal/apl/91/19?ver=pdfcov>

Published by the [AIP Publishing](#)



Re-register for Table of Content Alerts

Create a profile.



Sign up today!



Growth front nucleation of rubrene thin films for high mobility organic transistors

C. H. Hsu

School of Physics and Astronomy, University of Nottingham, Nottingham NG7 2RD, United Kingdom

J. Deng

School of Physics and Astronomy, University of Nottingham, Nottingham NG7 2RD, United Kingdom and School of Applied Mathematics and Physics, Beijing University of Technology, Beijing 100022, China

C. R. Staddon and P. H. Beton^{a)}

School of Physics and Astronomy, University of Nottingham, Nottingham NG7 2RD, United Kingdom

(Received 10 August 2007; accepted 12 October 2007; published online 7 November 2007)

We demonstrate a mode of thin film growth in which amorphous islands crystallize into highly oriented platelets. A cascade of crystallization is observed, in which platelets growing outward from a central nucleation point impinge on neighboring amorphous islands and provide a seed for further nucleation. Through control of growth parameters, it is possible to produce high quality thin films which are well suited to the formation of organic transistors. We demonstrate this through the fabrication of rubrene thin film transistors with high carrier mobility. © 2007 American Institute of Physics. [DOI: 10.1063/1.2805030]

The fundamental processes which control the growth of sublimed organic thin films are currently highly topical due to the great promise of these materials for technological applications. Thin films of organic molecules such as pentacene may be used to fabricate organic transistors that are compatible with flexible substrates and have carrier mobilities which are comparable to or higher than amorphous silicon.^{1–7} The performance of these devices is intimately related to the morphology of the polycrystalline thin films used to fabricate them, and these properties are, in turn, determined by the kinetics of nucleation and growth. Optimization of growth parameters for organic thin film transistors are focussed on maximizing the polycrystallite dimensions, thus minimizing unwanted grain boundary scattering, and the elimination of traps at the interface between the gate dielectric and organic channel.^{8,9}

The works of Podzorov *et al.*^{10–13} and Stassen *et al.*¹⁴ have led to the identification of rubrene as a material of particular promise for thin film organic transistors. However, attempts to grow thin film rubrene transistors have had only limited success since rubrene, when sublimed, grows in an amorphous phase. Devices based on such films initially yielded very low carrier mobilities of $\sim 10^{-6}$ cm²/V s.¹⁵ There has been progress in growing high quality crystalline, or polycrystalline, material using high overpressures of rubrene¹⁶ and organic heterolayers,¹⁷ and these approaches have led to higher values of carrier mobility which are as high as 10⁻² cm²/V s.¹⁸

In this paper, we report a mode of rubrene growth which yields highly oriented crystalline platelets on which high mobility organic transistors may be fabricated. Our experiments are undertaken using *p*-type Si(100) substrates with a thermally grown SiO₂ layer (typical thickness of 300 nm) which is passivated by exposure to octadecyltrimethylsilane (OTS).^{19,20} This treatment yields a highly hydrophobic surface with water droplets forming a typical static contact

angle of $\sim 104 \pm 3^\circ$. Rubrene is sublimed at rates in the range of 0.4–0.6 nm/min in a vacuum system with a base pressure of $\sim 10^{-7}$ Torr.

In the absence of the OTS passivating layer, or at low growth temperature, we observe a morphology which is highly reminiscent of spherulite growth in common with other groups.^{21,22} Images of such structures [acquired using atomic force microscopy (AFM)] show that these islands have a polycrystalline structure with needlelike crystals which splay out from a central point. Although the “spherulitic” islands are polycrystalline, the local orientation of the needlelike crystals can be highly correlated over length scales of up to ~ 0.5 mm. This morphology is closely related to growth front nucleation as discussed (for homogeneous films) by Granasy *et al.*,²³ and may be understood in terms of a nucleation event at the center of the island which then propagates outward by seeding further nucleation.

This mode of growth may be exploited to optimize morphology for transistor fabrication by combining the OTS passivation layer with a substrate temperature during growth of 80–85 °C. An AFM image (tapping mode) of rubrene islands in the early stages of growth at 80 °C is shown in Fig. 1(a). The average island diameter and separation are 4 and 7 μm, respectively, and the overall morphology is similar to that observed in the growth of other amorphous organic thin films.²⁴ Figure 1(b) shows an AFM image of a part of the surface where the islands have undergone a transformation to a polycrystalline form and where small platelets, with a typical height of ~ 50 nm, grow across the surface. It is clear that the islands in the surrounding region have retained their non-faceted amorphous shape, while those which are connected with the network of platelets have been converted into a polycrystalline form. An optical micrograph of a similar region is shown in Fig. 1(c).

We have found that by ramping the growth temperature slowly during the deposition, it is possible to grow samples on which large regions of the surface are almost completely covered with well ordered crystalline platelets, which are reminiscent of the films reported by Stingelin-Stutzmann

^{a)}Electronic mail: peter.betton@nottingham.ac.uk

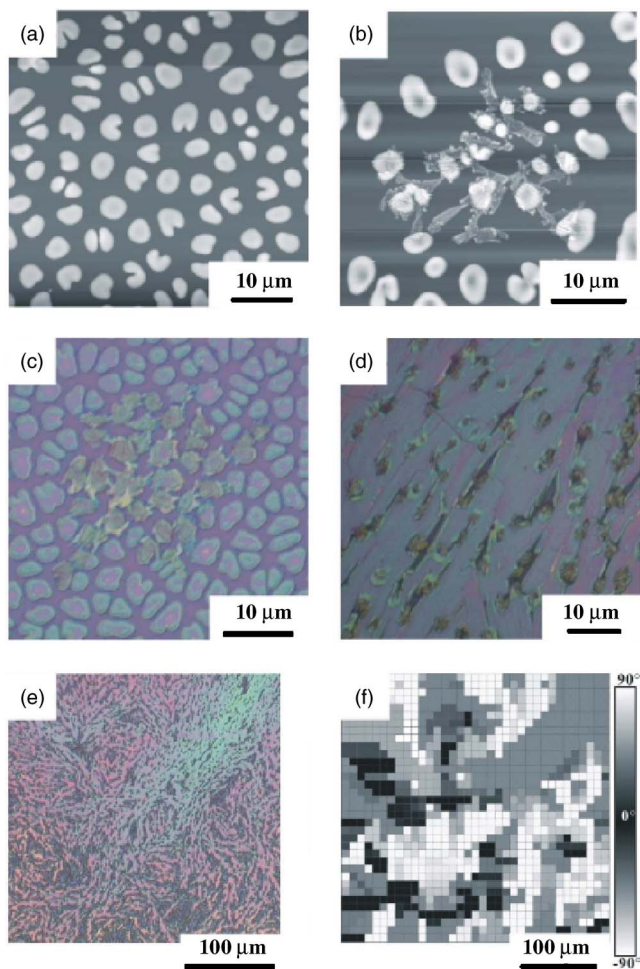


FIG. 1. (Color online) Rubrene polycrystalline thin films grown on an OTS treated substrate by ramping substrate temperature from 75 to 80 °C and deposition rate of 0.5 nm/min at different growth stages. (a) AFM image of isolated amorphous islands (deposition time of ~60 min). (b) AFM image of polycrystalline structure (deposition time of 80–100 min). (c) Optical micrograph of polycrystalline structure. (d) Optical micrograph of dense polycrystalline thin films (deposition time 320 min). (e) Optical micrograph of dense polycrystalline thin films (320–380 min). (f) Gray scale map of (e); contrast bar indicates facet angle orientation where 0° refers to x axis, while ±90° refers to y axis.

*et al.*²⁵ Optical images are shown in Figs. 1(d) and 1(e). The dimensions of typical platelets are $\sim 5 \times 30 \mu\text{m}^2$ and the direction of growth of neighboring crystallites is highly correlated. We observe grain boundaries running approximately diagonally from top right to bottom left in Fig. 1(d). We have analyzed the spatial variation of the orientation of crystallites for the layer shown in Fig. 1(e). The results are summarized in Fig. 1(f) where the orientational dependence is presented as a gray scale map. The orientation of crystallites is clearly correlated over distances of $>100 \mu\text{m}$, and in some regions (e.g., top right) up to $250 \mu\text{m}$.

Images of similar films acquired using AFM are shown in Figs. 2(a) and 2(b). In the lower magnification image [Fig. 2(a)], grain boundaries are evident running from top right to bottom left. Higher magnification images [Fig. 2(b)] show clear facets and terraced islands. Also observed are dark lines which run across the terrace structure [also observed in Fig. 2(a)]. Noting the continuity of the terrace structure on either side of these lines, we attribute them to cracks in the film which are probably formed when cooling the sample after growth.

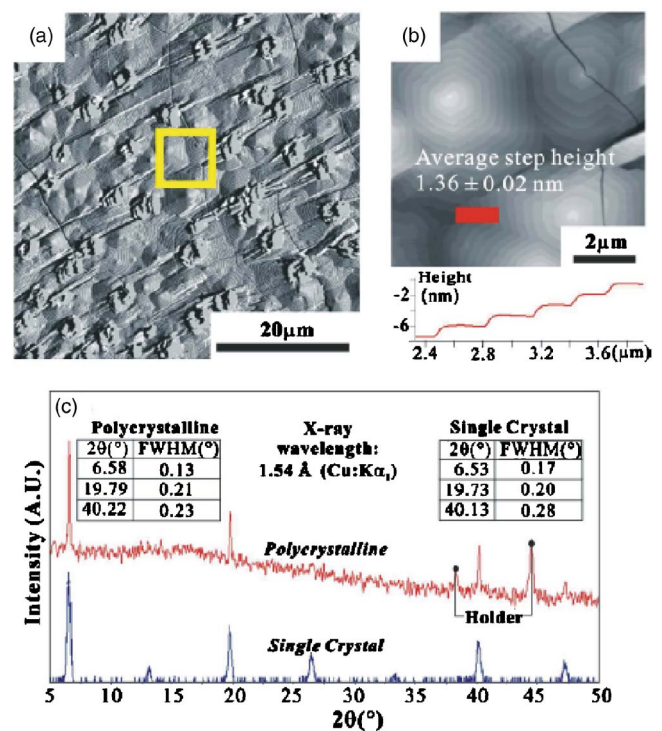


FIG. 2. (Color online) (a) AFM image (error signal) of rubrene thin films grown on OTS treated SiO₂ using conditions described in Fig. 2. (b) Zoom (topograph) of area in (a), with the cross sectional profile demonstrating step and terrace structures of the film. (c) XRD data for rubrene single crystal and thin film.

The crystallinity of the resulting films has been investigated using x-ray diffraction [Fig. 2(d)]. We observe clear peaks corresponding to the expected layer separation for planar growth of rubrene crystals with the [100] direction perpendicular to the substrate. The values for the position and half width of the peaks are very close to the values observed for x-ray diffraction from a rubrene single crystal grown by thermal gradient sublimation in our laboratory [see Fig. 3(c)] and those previously published.²⁶ The layer separation giving rise to the peak at $2\theta=6.58^\circ$ is 1.35 nm in close agreement with the terrace step height extracted from our AFM images (1.36 nm).

We have explored the potential of organic transistors based on thin films grown under these conditions. Figure 3 shows a schematic of the transistor geometry which is employed.²⁷ The Si substrate is used as a gate contact, and source and drain contacts are deposited on the rubrene thin film in a “top-contact” configuration with a measured gate capacitance C_g of 5.6 nF/cm². The source-drain gap is typically $\sim 10 \mu\text{m}$ and is defined using a shadow mask. The electrical characteristics of the transistors are measured under negative ambient conditions. We observe transistor action for negative gate biases corresponding to hole transport. The electrical characteristics of a high mobility device are shown in Fig. 3(a). An optical micrograph of the device is shown in Fig. 3(b). From these measurements, we deduce a value of hole mobility of 2.5 cm²/V s. This is comparable with the highest reported values for thin film organic transistors.^{1,4} Furthermore, we emphasize that in calculating the mobility, we have taken a value for the device width which corresponds to the physical dimensions of the device. In fact, there is clearly some inhomogeneity in the material which forms the channel, from which we deduce that the intrinsic

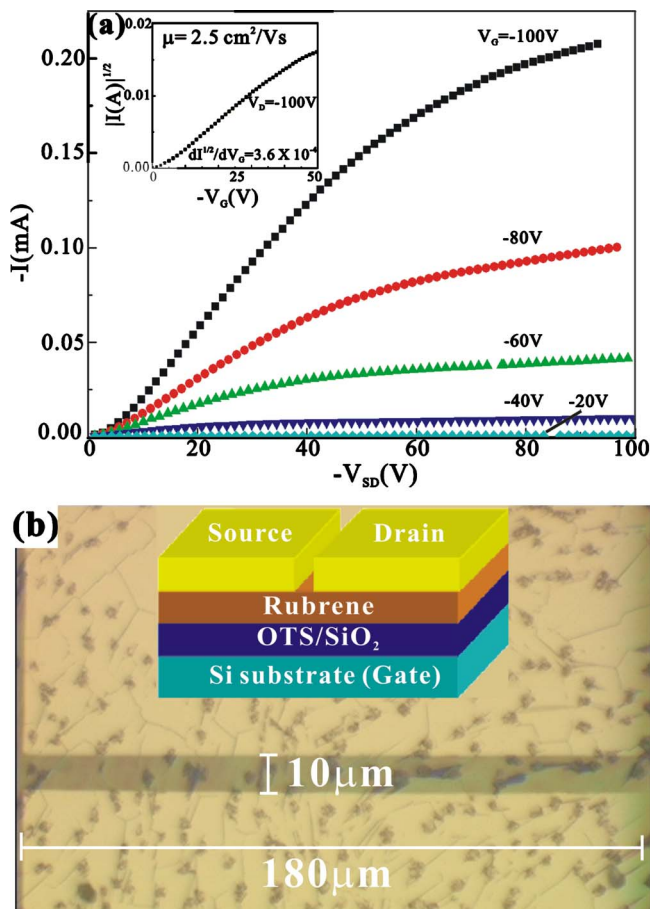


FIG. 3. (Color online) (a) I - V characteristics of a rubrene thin film field effect transistor (FET). Source-drain current I vs source-drain voltage V_{SD} measured at different values of gate voltage V_G ; inset: dependence of drain current I_D on gate voltage V_G for a fixed source-drain voltage of -100 V. (b) Optical micrograph of rubrene polycrystalline FET with gold source and drain contacts on the top. The inset illustrates the schematic of the device. Channel length and width are 10 and $180 \mu\text{m}$, respectively.

mobility of the material is considerably higher than the value quoted above.

We have fabricated many devices from thin films grown using this approach and find carrier mobilities ranging from 0.1 to $2.5 \text{ cm}^2/\text{V s}$. The value of mobility is correlated with the quality of the film within the transistor channel. For high quality films (i.e., those for which platelet crystallites almost entirely cover the source-drain gap), there is a further dependence on the orientation of the platelets. Specifically, mobility is higher for channels in which the long axis of the needlelike platelets is oriented parallel to the direction of current flow between the source and drain.

Our work shows that growth front nucleation in inhomogeneous thin films may be used to grow high quality organic thin films. Most importantly, this approach to growth offers a route to thin films, in which individual crystallites are much larger than the average separation of islands which are kinetically nucleated in the very early stages of growth. Furthermore, a correlation between the orientation of crystallites

over length scales approaching 0.5 mm confirms that the overall morphology of the film is not simply controlled by kinetic effects as observed, for example, in pentacene growth. Finally, we have shown that these thin films provide a route to the fabrication of high mobility organic transistors.

We acknowledge support from the UK Engineering and Physical Sciences Research Council (Grant No. GR/C534158). We are grateful to James Sharp for helpful discussions on spherulite growth.

- ¹S. F. Nelson, Y.-Y. Lin, D. J. Gundlach, and T. N. Jackson, *Appl. Phys. Lett.* **72**, 1854 (1998); C. D. Sheraw, L. Zhou, J. R. Huang, D. J. Gundlach, T. N. Jackson, M. G. Kane, I. G. Hill, M. S. Hammond, J. Campi, B. K. Greening, J. Francl, and J. West, *ibid.* **80**, 1088 (2002).
- ²R. Ruiz, D. Choudhary, B. Nickel, T. Toccoli, K. C. Chang, A. C. Mayer, P. Clancy, J. M. Blakely, R. L. Headrick, S. Iannotta, and G. G. Malliaras, *Chem. Mater.* **16**, 4497 (2004).
- ³H. E. Katz, *Chem. Mater.* **16**, 4748 (2004).
- ⁴H. Klauk, M. Halik, U. Zschieschang, G. Schmid, W. Radlik, and W. Weber, *J. Appl. Phys.* **92**, 5259 (2002).
- ⁵C. D. Dimitrakopoulos and P. R. L. Malenfant, *Adv. Mater. (Weinheim, Ger.)* **14**, 99 (2002).
- ⁶G. Wang, Y. Luo, and P. H. Beton, *Appl. Phys. Lett.* **83**, 3108 (2003).
- ⁷Y. Luo, G. Wang, J. A. Theobald, and P. H. Beton, *Surf. Sci.* **537**, 241 (2003).
- ⁸L. L. Chua, J. Zaumseil, J. F. Chang, E. C. W. Ou, P. K. H. Ho, H. Sirringhaus, and R. H. Friend, *Nature (London)* **434**, 194 (2005).
- ⁹F.-J. Meyer zu Heringdorf, M. C. Reuter, and R. M. Tromp, *Nature (London)* **412**, 517 (2001).
- ¹⁰V. Podzorov, V. M. Pudalov, and M. E. Gershenson, *Appl. Phys. Lett.* **82**, 1739 (2003).
- ¹¹V. Podzorov, S. E. Sysoev, E. Loginova, V. M. Pudalov, and M. E. Gershenson, *Appl. Phys. Lett.* **83**, 3504 (2003).
- ¹²V. C. Sundar, J. Zaumseil, V. Podzorov, E. Menard, R. L. Willett, T. Someya, M. E. Gershenson, and J. A. Rogers, *Science* **303**, 1644 (2004).
- ¹³R. W. I. de Boer, M. E. Gershenson, A. F. Morpurgo, and V. Podzorov, *Phys. Status Solidi A* **201**, 1302 (2004).
- ¹⁴A. F. Stassen, R. W. I. de Boer, N. N. Iosad, and A. F. Morpurgo, *Appl. Phys. Lett.* **85**, 3899 (2004).
- ¹⁵S. Seo, B. N. Park, and P. G. Evans, *Appl. Phys. Lett.* **88**, 232114 (2006).
- ¹⁶D. Kafer and G. Witte, *Phys. Chem. Chem. Phys.* **7**, 2850 (2005).
- ¹⁷J. H. Seo, D. S. Park, S. W. Cho, C. Y. Kim, W. C. Jang, C. N. Whang, K.-H. Yoo, G. S. Chang, T. Pedersen, A. Moewes, K. H. Chae, and S. J. Cho, *Appl. Phys. Lett.* **89**, 163505 (2006).
- ¹⁸S.-W. Park, S. H. Jeong, J.-M. Choi, J. M. Hwang, J. H. Kim, and S. Im, *Appl. Phys. Lett.* **91**, 033506 (2007).
- ¹⁹T. Komeda, K. Namba, and Y. Nishioka, *J. Vac. Sci. Technol. A* **16**, 3 (1998).
- ²⁰P. Silberzan, L. Leger, D. Ausserre, and J. J. Benattar, *Langmuir* **7**, 1647 (1991).
- ²¹Y. Luo, M. Brun, P. Rannou, and B. Grevin, *Phys. Status Solidi A* **204**, 1851 (2007).
- ²²M. Haemori, J. Yamaguchi, S. Yaginuma, K. Itaka, and H. Koinuma, *Jpn. J. Appl. Phys., Part 1* **44**, 6A (2005).
- ²³L. Granasy, T. Pusztai, T. Borzsonyi, J. A. Warren, and J. F. Douglas, *Nat. Mater.* **3**, 645 (2004).
- ²⁴M. Brinkmann, S. Graff, and F. Biscarini, *Phys. Rev. B* **66**, 165430 (2002).
- ²⁵N. Stingelin-Stutzmann, E. Smits, H. Wondergem, C. Tanase, P. Blom, P. Smith, and D. De Leeuw, *Nat. Mater.* **4**, 601 (2005).
- ²⁶D. E. Henn, *J. Appl. Crystallogr.* **4**, 256 (1971).
- ²⁷R. C. Haddon, A. S. Perel, R. C. Morris, T. C. M. Palstra, A. F. Hebard, and R. M. Fleming, *Appl. Phys. Lett.* **67**, 121 (1995).